

Shortcuts to adiabatic holonomic quantum computation in decoherence-free subspace with transitionless quantum driving algorithm*

Xue-Ke Song, Hao Zhang, Qing Ai, Jing Qiu, and Fu-Guo Deng[†]

Department of Physics, Applied Optics Beijing Area Major Laboratory, Beijing Normal University, Beijing 100875, China

(Dated: November 10, 2021)

By using transitionless quantum driving algorithm (TQDA), we present an efficient scheme for the shortcuts to the holonomic quantum computation (HQC). It works in decoherence-free subspace (DFS) and the adiabatic process can be speeded up in the shortest possible time. More interestingly, we give a physical implementation for our shortcuts to HQC with nitrogen-vacancy centers in diamonds dispersively coupled to a whispering-gallery mode microsphere cavity. It can be efficiently realized by controlling appropriately the frequencies of the external laser pulses. Also, our scheme has good scalability with more qubits. Different from previous works, we first use TQDA to realize a universal HQC in DFS, including not only two noncommuting accelerated single-qubit holonomic gates but also a accelerated two-qubit holonomic controlled-phase gate, which provides the necessary shortcuts for the complete set of gates required for universal quantum computation. Moreover, our experimentally realizable shortcuts require only two-body interactions, not four-body ones, and they work in the dispersive regime, which relax greatly the difficulty of their physical implementation in experiment. Our numerical calculations show that the present scheme is robust against decoherence with current experimental parameters.

PACS numbers: 03.67.Lx, 03.67.Pp, 03.65.Vf, 42.50.Pq

I. INTRODUCTION

Quantum computation (QC), which permits unitary operations on qubits, has attracted considerable attention in recent years [1]. Many interesting theoretical schemes have been proposed for universal quantum logic gates in various quantum systems, such as trapped ions [2], atom-cavity systems [3], photons [4, 5], quantum dots [6], circuit quantum electrodynamics [7], and so on. In experiment, there are stochastic control errors during the gate operation and the collective noise caused by the interaction between a quantum system and its ambient environment. To suppress the former, Zanardi and Rasetti [8] introduced the holonomic quantum computation (HQC) which is based on the adiabatic non-abelian geometric phases (holonomies) in 1999. The advantage of HQC is that it depends only on the global geometric properties of the evolution in parameter space, but resilience of the local noises and fluctuations [8, 9]. In 2001, Duan *et al.* [10] proposed an interesting scheme for adiabatic geometric QC in trapped ions. Subsequently, much effort was made on nonadiabatic geometric QC [11–21] and unconventional geometric QC [22–24]. These holonomic quantum gates are more robust than the conventional ones. Interestingly, the nonadiabatic geometric QC were demonstrated in several physical systems by some groups. For example, in 2013, Feng, Xu, and Long [25] experimentally realized the nonadiabatic HQC in a liquid NMR quantum information processor for the first time, including one-qubit holonomic gates and the two-qubit holonomic controlled-not gate. Meanwhile, Abdumalikov *et al.* [26] realized firstly the nonadiabatic holonomic single-qubit operations on a three-level transmon qubit. In 2014,

two groups [27, 28] demonstrated the nonadiabatic holonomic quantum gates in diamond nitrogen-vacancy (NV) centers.

The decoherence-free subspace (DFS) [29–31] of a quantum system can protect the fragile quantum information against collective noises as the system undergoes a unitary evolution in its DFS. It has been demonstrated that DFS can be implemented experimentally with different physical systems [32–34]. In 2005, Wu *et al.* [35] presented a theoretic scheme by combining the HQC and DFS to perform universal QC. By making the dark states of the Hamiltonian of a quantum system adiabatically evolve along a closed cyclic loop, one can acquire a Berry phase or quantum holonomy. In 2006, Zhang *et al.* [36] and Cen *et al.* [37] gave two schemes for HQC with DFS in trapped ions. In 2009, Oreshkov *et al.* [38] introduced a scheme for fault-tolerant HQC on stabilizer codes. The adiabatic evolution for HQC requires a long run time. To eliminate this dilemma, Berry [39] came up with a transitionless quantum driving algorithm (TQDA), which is also outlined in slightly different manner by Demirplak and Rice [40, 41], to speed up the adiabatic quantum gates when the eigenstates of a time-dependent Hamiltonian are non-degenerate in 2009. Later, this transitionless algorithm has been gained widespread attention in both theory and experiment [42–47]. In 2010, Chen *et al.* [42] used the TQDA to speed up adiabatic passage techniques in two-level and three-level atoms extending to the short-time domain their robustness with respect to parameter variations. In 2012, Bason *et al.* [46] experimentally implemented the optimal high-fidelity transitionless superadiabatic protocol on Bose-Einstein condensates in optical lattices. In 2013, Zhang *et al.* [47] implemented the acceleration of quantum adiabatic passages on the electron spin of a single NV center in diamond. As for the degenerate case, Zhang *et al.* [48] generalized TQDA to show the adiabatic shortcuts to holonomic quantum gates without DFS. In 2015, Pyshkin *et al.* [49] showed that the conventional HQC can be accelerated by using external control fields.

*Published in New J. Phys. **18**, 023001 (2016)

[†]Corresponding author: fgdeng@bnu.edu.cn

Recently, the diamond NV center coupled to a quantized whispering-gallery mode (WGM) of a fused-silica high-Q microcavity has been extensively investigated in quantum information. On one hand, an NV center in a diamond has long electron-spin coherence time even at room temperature [50], and it is easy to manipulate, initialize, and readout the quantum state on the NV center via the external laser and microwave field [27, 28]. On the other hand, a microcavity can attain a ultrahigh Q factor ($>10^8$ even up to 10^{10}) with a very small volume [51, 52]. Taking advantage of the exceptional spin features of NV centers and the ultrahigh-Q factor of microsphere cavity, Park *et al.* [53] observed the normal mode splitting in this cavity QED system in 2006. Afterward, some interesting schemes for high-fidelity entanglement generation between separate NV centers and other quantum information tasks have been proposed [54–57]. In 2010, Yang *et al.* [54] proposed a scheme for generating the W state and Bell state in this nanocrystal-microsphere system. In 2015, Ren *et al.* [56] presented the dipole induced transparency of an NV center embedded in a photonic crystal cavity coupled to two waveguides and designed two universal hyperparallel hybrid photonic quantum logic gates. Liu and Zhang [57] proposed two efficient schemes for the deterministic generation and the complete nondestructive analysis of hyperentangled Bell states, assisted by the NV centers coupled to microtoroidal resonators.

In this paper, we propose an efficient scheme to speed up the adiabatic holonomic quantum gates in DFS by using TQDA. This proposal takes advantage of the fault tolerance of HQC and coherence preserving virtues of DFS to protect quantum information from local fluctuations and collective noises. The TQDA makes the adiabatic holonomic quantum process be accelerated in the shortest possible time. In addition, we present a feasible physical implementation of this protocol with diamond NV centers dispersively coupled to a quantized WGM of a microsphere cavity. We can achieve the shortcuts to adiabatic HQC in DFS by tuning the frequencies of the external laser field, which simplifies the operation procedure largely. Our scheme is scalable as it can be straightforwardly applied to HQC with multiple qubits. Different from previous works, we use TQDA to realize a universal HQC in DFS, including both two noncommuting accelerated single-qubit holonomic gates and a accelerated two-qubit holonomic controlled-phase (CP) gate. This provides an efficient route for shortcuts to adiabatic HQC in DFS. Moreover, the present proposal requires only two-body interaction, not four-body ones, which largely reduces the experimental challenge. With a virtual photon process, the cavity decay is greatly suppressed. Our numerical calculations show that this scheme can reach a high fidelity with current experiment parameters, and it exhibits the robustness of the HQC.

II. BASIC THEORIES

Let us give a brief review of TQDA for a general quantum system with an arbitrary time-dependent Hamiltonian $H_0(t)$. If the initial state is in one of the eigenstates of the Hamil-

tonian $H_0(t)$, the quantum adiabatic theorem guarantees that the system remains approximately in this eigenstate when the time evolution is sufficiently slow. Due to the long runtime required for adiabatic evolution, it will bring in the extra loss of coherence and spontaneous emission of the quantum system. In 2009, Berry [39] introduced an optimized quantum algorithm, i.e., TQDA, to speed up the adiabatic process. Actually, the main idea of TQDA is that if the adiabatic approximation for the evolution operator of a given quantum system is specified, one can find another Hamiltonian $H(t)$ which can generate the equivalent unitary transformation in a shortest possible time. In the TQDA, the Hamiltonian $H(t)$ drives the evolving states following the selected instantaneous adiabatic eigenstates of $H_0(t)$ exactly without undergoing transitions, while there is no limitation to the adiabatic theorem. The Hamiltonian $H(t)$ can be divided into two parts: one is the fundamental Hamiltonian $H_0(t)$ for adiabatic evolution, and the other is the additional Hamiltonian $H_1(t)$ which can suppress the transitions of the system due to the rapid evolution. In theory, the TQDA ensures that the state of the quantum system remains in the eigenstate of the Hamiltonian $H_0(t)$ invariable for all time. This reveals that the adiabatic evolution can be accelerated close to the quantum speed limit by using the TQDA [46].

More specifically, considering the fundamental Hamiltonian $H_0(t)$ of the quantum system has the non-degenerate instantaneous eigenstates $|n(t)\rangle$ with corresponding eigenvalues $E_n(t)$, in the adiabatic approximation, one could write the state evolution of the system by

$$|\Psi_n(t)\rangle = \exp\left\{-i\int_0^t dt' E_n(t') - \int_0^t dt' \langle n(t')|\dot{n}(t')\rangle\right\}|n(t)\rangle. \quad (1)$$

By employing the reverse engineering approach described in Ref. [39], the driving Hamiltonian $H(t)$, with $\hbar = 1$, takes the form of

$$H(t) = \sum_n E_n |n\rangle\langle n| + i \sum_n (|\dot{n}\rangle\langle n| - \langle n|\dot{n}\rangle|n\rangle\langle n|) = H_0(t) + H_1(t), \quad (2)$$

where all kets are time-dependent and $H_0(t) = \sum_n E_n |n\rangle\langle n|$.

On the other hand, if there exists degeneracy in the spectrum of the Hamiltonian, the situation becomes more complex and troublesome. To get rid of this dilemma, Zhang *et al.* [48] generalized the non-degenerate TQDA to the degenerate case, which can acquire non-Abelian geometric phases, i.e., quantum holonomies, after a cyclic evolution. Likewise, the transitionless driving Hamiltonian to achieve adiabatic shortcuts for the degenerate case is given by

$$\begin{aligned} H'(t) &= \sum_{n,k} E_n |\varphi_k^n\rangle\langle\varphi_k^n| + \sum_n \left(i |\dot{\varphi}_k^n\rangle\langle\varphi_k^n| - A_{kl}^n |\varphi_k^n\rangle\langle\varphi_l^n| \right) \\ &= H'_0(t) + H'_1(t), \end{aligned} \quad (3)$$

in which $H'_0(t) = \sum_{n,k} E_n |\varphi_k^n\rangle\langle\varphi_k^n|$, $|\varphi_k^n\rangle$ ($k = 1, 2, \dots, m_n$) are a set of degenerate eigenstates with the corresponding eigenvalues $E_n(t)$ of the Hamiltonian $H'_0(t)$, and $A_{kl}^n = i \langle\varphi_k^n|\dot{\varphi}_l^n\rangle$ represents the matrix-valued connection, also known as the holonomy matrix.

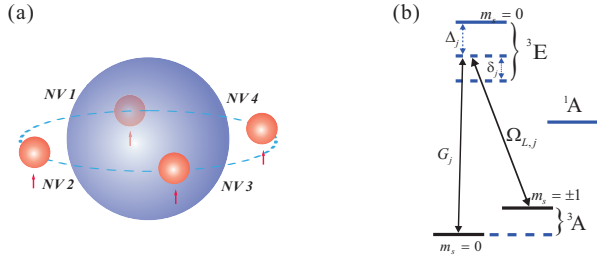


FIG. 1: (a) Schematic diagram for N identical NV centers locating around the equator of a fused-silica microsphere cavity. (b) The energy-level configuration for an NV center, where Δ_j and δ_j are the detunings, G_j and $\Omega_{L,j}$ are the coupling strength between an NV center and a quantized WGM of the microsphere cavity and that between an NV center and the external laser field, respectively. Here, the states $|^3A, m_s = 0\rangle$, $|^3A, m_s = -1\rangle$ and $|^3E, m_s = 0\rangle$ are encoded as the qubit states $|0\rangle$, $|1\rangle$, and $|e\rangle$, respectively.

III. EFFECTIVE HAMILTONIAN BASED ON NV CENTERS INTERACTING WITH MICROSPHERE RESONATOR

Our system is composed of N identical NV centers in N separate diamond nanocrystals which are dispersively coupled to a quantized WGM at the equator of single fused-silica microsphere cavity, respectively, shown in Fig. 1(a). An NV center consists of a substitutional nitrogen atom and an adjacent vacancy in diamond lattice, and it can be easily manipulated by optical and microwave field. By imposing laser pulses on the arbitrary NV center interacting with the WGM, the NV center can be modeled as a Λ -type three-level structure, as shown in Fig. 1(b), where the states $|^3A, m_s = 0\rangle$ and $|^3A, m_s = -1\rangle$ are labeled by the qubit states $|0\rangle$ and $|1\rangle$, respectively. $|^3E, m_s = 0\rangle$ serves as the excited state $|e\rangle$. In our scheme, the transition $|0\rangle \leftrightarrow |e\rangle$ with the frequency ω_{e0} is far-off resonant with the WGM whose frequency is ω_c , and $|1\rangle \leftrightarrow |e\rangle$ with the frequency ω_{e1} is driven by a largely detuned classical laser field with the frequency ω_L and the polarization σ^+ [58]. Assuming both the coupling strengths G_j and $\Omega_{L,j}$ are sufficiently smaller than the detuning Δ_j , the state $|e\rangle$ can be adiabatically eliminated. The NV centers are fixed and separated by distance much larger than the wavelength of the WGM, so that there are no the direct coupling among NV centers, and they can interact with laser beams individually. Under the rotating wave approximation, the interaction Hamiltonian, in the interaction picture, can be expressed as

$$H_{int} = \sum_{j=1}^N g_j a \sigma_j^+ e^{-i(\delta_j t - \phi_j)} + H.c., \quad (4)$$

where a^+ (a) is the creation (annihilation) operator for the WGM, ϕ_j is initial phase of the laser field imposed on the j -th NV center, $\sigma_j^+ = |1\rangle_j \langle 0|$, $\sigma_j^- = |0\rangle_j \langle 1|$, and the coupling strength $g_j = G_j \Omega_{L,j} \left(\frac{1}{\Delta_j + \delta_j} + \frac{1}{\Delta_j} \right)$ with $\Delta_j = \omega_{e0,j} - \omega_c$, $\delta_j = \omega_c - \omega_{10,j} - \omega_{L,j}$, and $\omega_{10,j} = \omega_{e0,j} - \omega_{e1,j}$.

To take $\delta_j \gg g_j$ into account, i.e., in the dispersive regime, the direct energy exchange between NV centers and WGM is negligible. Using the unitary transformation $U = \exp\left[\frac{g}{\delta}(a^+ \sigma^- - a \sigma^+)\right]$ to eliminate the direct NV-center-WGM coupling, one can obtain the effective Hamiltonian for the system composed of the NV centers as follows:

$$H_{eff} = \sum_{j=1}^N \frac{g_j^2}{\delta_j} a a^+ |1\rangle_j \langle 1| + \sum_{j,k,j \neq k}^N \lambda_{j,k} \left(e^{i\phi_{jk}} \sigma_j^- \sigma_k^+ + H.c. \right), \quad (5)$$

where $\lambda_{j,k} = \frac{g_j g_k}{2} \left(\frac{1}{\delta_j} + \frac{1}{\delta_k} \right)$ and $\phi_{jk} = \phi_j - \phi_k$. Here we assume the WGM field is initially in the vacuum state. The first term corresponds to the Stark shift term, which can be compensated by applying additional lasers with appropriate frequencies [59, 60]. For simplicity, hereafter, we assume that the coupling strengths g_j ($j = 1, 2, \dots$) are identical for all the NV centers, that is, $g_j = g_k = g$. The effective Hamiltonian can be further simplified as

$$H'_{eff} = \sum_{j,k,j \neq k}^N \lambda'_{j,k} \left(e^{i\phi_{jk}} \sigma_j^- \sigma_k^+ + H.c. \right), \quad (6)$$

where $\lambda'_{j,k} = \frac{g^2}{2} \left(\frac{1}{\delta_j} + \frac{1}{\delta_k} \right)$, which serves as the effective Rabi frequency for the energy conservation transition between the j -th and k -th NV centers. It is indicated that the Rabi frequency $\lambda'_{j,k}$ is inversely proportional to the detuning δ_j (δ_k), which relies largely on the difference between the frequencies of cavity field ω_c and the external laser field $\omega_{L,j}$ ($\omega_{L,k}$). With the Hamiltonian H'_{eff} , applying different initial conditions, one can achieve efficiently the shortcuts to the adiabatic single-logic-qubit gates and the two-logic-qubit gate in DFS on this NV-center system, and the detailed physical implementation about it will be presented in next Section.

IV. SHORTCUTS TO ADIABATIC SINGLE-QUBIT HOLONOMIC GATES IN DFS WITH NV CENTERS SYSTEM

A. Shortcuts to adiabatic single-qubit bit-phase gate in DFS

Considering a four-NV-center system which is coupled to a microsphere resonator in a symmetric way and undergoes a dephasing process, described by the interaction Hamiltonian $H_I = \sum_{i=1}^4 \sigma_z^i \otimes B$, where B is an arbitrary environment operator. The DFS against the collective dephasing noise can be expressed as $C_1 := \text{span}\{|0001\rangle, |0010\rangle, |0100\rangle, |1000\rangle\}$, in which $|0\rangle_L = |0001\rangle$ and $|1\rangle_L = |0010\rangle$ denote the computational basis, and the remaining states $|a_1\rangle = |1000\rangle$ and $|a_2\rangle = |0100\rangle$ are employed as the ancillary states. For accomplishing the single-qubit bit-phase gate in this logical DFS, we can utilize the target Hamiltonian

$$H_0^y(t) = \lambda'_{1,4} |a_1\rangle_L \langle 0| + \lambda'_{1,3} |a_1\rangle_L \langle 1| + \lambda'_{1,2} |a_1\rangle \langle a_2| + H.c., \quad (7)$$

where $\lambda'_{j,k}$ is the effective coupling strength between the j -th and k -th NV centers for this four-NV-center system, $\lambda'_{1,4} =$

$\lambda' \sin \theta \cos \varphi$, $\lambda'_{1,3} = \lambda' \sin \theta \sin \varphi$, $\lambda'_{1,2} = \lambda' \cos \theta$ with $\lambda' = \sqrt{|\lambda'_{1,2}|^2 + |\lambda'_{1,3}|^2 + |\lambda'_{1,4}|^2}$, and θ and φ are the time-dependent tunable parameters with $\theta \in [0, \pi]$ and $\varphi \in [0, 2\pi]$. The dark states of the Hamiltonian $H_0^y(t)$ are $|D_0^y(t)\rangle = \cos \theta \cos \varphi |0\rangle_L + \cos \theta \sin \varphi |1\rangle_L - \sin \theta |a_2\rangle$ and $|D_1^y(t)\rangle = -\sin \varphi |0\rangle_L + \cos \varphi |1\rangle_L$, respectively. Under the adiabatic cyclic evolution of the dark states, one gets the required single-qubit holonomic bit-phase gate $U_y = e^{i\beta_2 \sigma^y}$, where $\sigma^y = i(|0\rangle_L \langle 1| - |1\rangle_L \langle 0|)$ and β_2 is the Berry phase factor. As shown in Eq. (3), it is known that with the purpose of achieving shortcuts to the adiabatic gate U_y , one needs an additional Hamiltonian $H_1^y(t)$ that can block the transition of quantum states caused by the rapid evolution of the system. In the ordered orthogonal basis $\{|a_1\rangle, |0\rangle_L, |1\rangle_L, |a_2\rangle\}$, the additional Hamiltonian for speeding up the adiabatic single-qubit holonomic bit-phase gate U_y reads

$$H_1^y(t) = i \cos \theta \dot{\varphi} \begin{pmatrix} 0 & 0 & 0 & 0 \\ 0 & 0 & \cos \theta & -\sin \theta \sin \varphi \\ 0 & -\cos \theta & 0 & \sin \theta \cos \varphi \\ 0 & \sin \theta \sin \varphi & -\sin \theta \cos \varphi & 0 \end{pmatrix} + i \begin{pmatrix} 0 & 0 & 0 & 0 \\ 0 & 0 & -\dot{\varphi} & \cos \varphi \dot{\theta} \\ 0 & \dot{\varphi} & 0 & \sin \varphi \dot{\theta} \\ 0 & -\cos \varphi \dot{\theta} & -\sin \varphi \dot{\theta} & 0 \end{pmatrix}. \quad (8)$$

Now, we focus on how to realize the shortcuts to the adiabatic single-logic-qubit bit-phase gate U_y on the four-NV-center system by making use of the additional Hamiltonian. In this case, we choose the initial phase difference between the external classical laser pulses $\phi_{jk} = 0$. On the first step, setting $\varphi = 0$, while increasing θ from 0 to $\pi/2$, the corresponding Hamiltonian of the system in the DFS C_1 is $H^{y1} = \lambda' \sin \theta |a_1\rangle_L \langle 0| + \lambda' \cos \theta |a_1\rangle_L \langle a_2| + i \dot{\theta} |0\rangle_L \langle a_2| + H.c..$ This Hamiltonian is under a Δ -style structure. For achieving this goal, we can tune the effective Rabi frequencies between the physical qubits as $\lambda'_{1,4} = \lambda' \sin \theta$, $\lambda'_{1,2} = \lambda' \cos \theta$, and $\lambda'_{2,4} = \dot{\theta}$, and other control parameters are zero. In other words, the first step can be effectively completed by the three laser fields with different frequencies being applied to the 1-st, 2-nd, and 4-th NV centers, while there is no any operation on 3-th NV center when the cavity frequency is constant. Second, keeping θ invariant but changing φ from 0 to a certain value φ_c , the required Hamiltonian takes the form of $H^{y2} = \lambda' \cos \varphi |a_1\rangle_L \langle 0| + \lambda' \sin \varphi |a_1\rangle_L \langle 1| - i \dot{\varphi} |0\rangle_L \langle 1| + H.c..$ Adjusting the effective Rabi frequencies $\lambda_{1,4} = \lambda' \cos \varphi$, $\lambda_{1,3} = \lambda' \sin \varphi$, and $\lambda_{3,4} = \dot{\varphi}$, one can obtain the required Hamiltonian. It is worth emphasizing that the minimal resources with three different frequencies of the external laser pulse can achieve the second step. Finally, we keep φ unchanged while decrease θ to 0. The control Hamiltonian for this case reads $H^{y3} = \lambda' \sin \theta \cos \varphi |a_1\rangle_L \langle 0| + \lambda' \sin \theta \sin \varphi |a_1\rangle_L \langle 1| + \lambda' \cos \theta |a_1\rangle_L \langle a_2| + i \dot{\theta} \cos \varphi |0\rangle_L \langle a_2| + i \dot{\theta} \sin \varphi |1\rangle_L \langle a_2| + H.c.,$ and then the system forms a cyclic evolution after tuning φ to 0. Different from the former two steps, in order to realize the last step, all of the four NV centers should be imposed on the external laser pulse with different frequencies to obtain the different effective Rabi frequencies $\lambda'_{j,k}$ ($j, k = 1, 2, 3, 4$, and

$j \neq k$). The details for the parameters chosen in each step for speeding up the adiabatic U_y gate are shown in Table I. Up to now, we have implemented the shortcuts to the single-logic-qubit holonomic bit-phase gate on the four-NV-center system in DFS.

TABLE I: Scheme for a three-step approach to realize the shortcuts to the adiabatic holonomic single-qubit bit-phase gate.

Step	θ	φ	the required Hamiltonian
(i)	$0 \rightarrow \pi/2$	0	H^{y1}
(ii)	$\pi/2$	$0 \rightarrow \varphi_c$	H^{y2}
(iii)	φ_c	$\pi/2 \rightarrow 0$	H^{y3}

B. Shortcuts to adiabatic single-qubit phase gate in DFS

Here, we illustrate how to accelerate another holonomic gate, phase gate, which is noncommuted with the single-qubit bit-phase gate. The target Hamiltonian in the same DFS C_1 can be designed as

$$H_0^z(t) = \lambda'_{1,3} e^{i\phi} |a_1\rangle_L \langle 1| + \lambda'_{1,2} |a_1\rangle_L \langle a_2| + H.c., \quad (9)$$

where $\lambda' = \sqrt{|\lambda'_{1,2}|^2 + |\lambda'_{1,3}|^2}$, and the relative phase $\theta = 2 \arctan(|\lambda'_{1,3}|/|\lambda'_{1,2}|)$ and ϕ are the time-dependent control parameters with $\theta \in [0, \pi]$ and $\phi \in [0, 2\pi]$. The Hamiltonian $H_0^z(t)$ has two degenerate dark states as $|D_0(t)\rangle = |0\rangle_L$ and $|D_1(t)\rangle = \cos \frac{\theta}{2} |1\rangle_L - \sin \frac{\theta}{2} e^{i\phi} |a_2\rangle$, in company with two non-degenerate bright states. In the dark-state subspace, we set $\theta = \phi = 0$ initially. Using the standard formula for the HQC, we can get the single-qubit holonomic phase gate $U_z = e^{i\beta_1 |1\rangle_L \langle 1|}$ by adiabatically changing the angles θ and ϕ after a cyclic evolution, where $\beta_1 = -\oint \sin^2 \frac{\theta}{2} d\phi$, corresponding to half the solid angle swept out by the polar angles θ and ϕ . Thus, we can obtain the additional control Hamiltonian $H_1^z(t)$ to realize the shortcuts to the holonomic phase gate U_z with the basis $\{|a_1\rangle, |1\rangle_L, |a_2\rangle\}$. That is,

$$H_1^z(t) = \frac{\dot{\phi}}{2} \sin^2 \frac{\theta}{2} \begin{pmatrix} -1 & 0 & 0 \\ 0 & 3 \cos^2 \frac{\theta}{2} - 1 & -\frac{3}{2} \sin \theta e^{-i\phi} \\ 0 & -\frac{3}{2} \sin \theta e^{i\phi} & 3 \sin^2 \frac{\theta}{2} - 1 \end{pmatrix} + \begin{pmatrix} 0 & 0 & 0 \\ 0 & \sin^2 \frac{\theta}{2} \dot{\phi} & \frac{1}{2} e^{-i\phi} (i\dot{\theta} + \sin \theta \dot{\phi}) \\ 0 & \frac{1}{2} e^{i\phi} (-i\dot{\theta} + \sin \theta \dot{\phi}) & -\sin^2 \frac{\theta}{2} \dot{\phi} \end{pmatrix}. \quad (10)$$

Similar to the approach for the shortcuts to single-logic-qubit adiabatic bit-phase gate, we can also accelerate the adiabatic single-logic-qubit phase gate U_z . It can be summarized as follows: (i) choosing $\phi = 0$, while changing θ from 0 to π , the corresponding Hamiltonian can be written by $H^{z1} = \lambda' \sin \frac{\theta}{2} |a_1\rangle_L \langle 1| + \lambda' \cos \frac{\theta}{2} |a_1\rangle_L \langle a_2| + \frac{1}{2} i \dot{\theta} |1\rangle_L \langle a_2| + H.c.;$ (ii) keeping $\theta = \pi$, but increasing ϕ from 0 to ϕ_c , and the required Hamiltonian is $H^{z2} = \lambda' e^{i\phi} |a_1\rangle_L \langle 1| + \lambda' e^{-i\phi} |1\rangle_L \langle a_1| -$

$\frac{\phi}{2}|a_1\rangle_L\langle a_1| + \frac{\phi}{2}|1\rangle\langle 1|$; (iii) setting ϕ unchanged, while decreasing θ to 0, and the required Hamiltonian takes the form of $H^{z3} = \lambda' \sin \frac{\theta}{2} e^{i\phi} |a_1\rangle_L\langle 1| + \lambda' \cos \frac{\theta}{2} |a_1\rangle_L\langle a_2| + \frac{1}{2} i \theta e^{-i\phi} |1\rangle_L\langle a_2| + H.c.$. The detailed steps for shortcuts to the phase gate are shown in Table II, in which the dark eigenstates of $H_0^z(t)$ complete a cyclic evolution in the parameter space. Apparently, the cyclic evolution path of this approach is unlike the one in the shortcuts to the adiabatic holonomic single-logic-qubit bit-phase gate U_y . On the other hand, the quantum operations involved for realizing the accelerated phase gate, which only require three of the four NV centers at most to be imposed the external classical laser pulses, are much simpler than the case in the bit-phase gate. The experimental complexity is greatly reduced. Based on the analysis, it is not difficult to find that as long as the cavity frequency and the initial phase of the external laser field are fixed, one can tune the different frequency of the external laser pulse to achieve the shortcuts to the adiabatic single-logic-qubit phase gate U_z in DFS.

TABLE II: Scheme for a three-step approach to realize the shortcuts to the adiabatic holonomic single-qubit phase gate.

Step	θ	ϕ	the required Hamiltonian
(i)	$0 \rightarrow \pi$	0	H^{z1}
(ii)	π	$0 \rightarrow \phi_c$	H^{z2}
(iii)	ϕ_c	$\pi \rightarrow 0$	H^{z3}

V. SHORTCUTS TO ADIABATIC TWO-QUBIT HOLONOMIC CP GATE IN DFS WITH NV CENTERS SYSTEM

Our shortcuts scheme for adiabatic two-qubit holonomic CP gate, which is a more basic and crucial element for a universal holonomic quantum computer, is based on a variant of the proposed HQC on the DFS in Ref. [35]. To this end, one needs eight physical qubits to encode two logical qubits. We define four computational states as $|00\rangle_L = |00010001\rangle$, $|01\rangle_L = |00010010\rangle$, $|10\rangle_L = |00100001\rangle$ and $|11\rangle_L = |00100010\rangle$, with two ancillary states $|a_3\rangle = |10000010\rangle$ and $|a_4\rangle = |01000010\rangle$. When the physical qubits interact collectively with the dephasing environment, the DFS can be chosen as $C_2 := \text{span}\{|00\rangle_L, |01\rangle_L, |10\rangle_L, |11\rangle_L, |a_3\rangle, |a_4\rangle\}$, and the target Hamiltonian takes the form as follows:

$$H_0^{cz}(t) = \lambda'_{1,3} e^{i\phi} |a_3\rangle_L\langle 11| + \lambda'_{1,2} |a_3\rangle\langle a_4| + H.c. \quad (11)$$

Here the parameters $\lambda'_{1,3}$, $\lambda'_{1,2}$, and ϕ have the same forms as those in the case for the single-qubit holonomic phase gate. It is straightforward to obtain the eigenstates with zero eigenvalue of the Hamiltonian as follows: $|D_0''(t)\rangle = |00\rangle_L$, $|D_1''(t)\rangle = |01\rangle_L$, $|D_2''(t)\rangle = |10\rangle_L$, and $|D_3''(t)\rangle = \cos \frac{\theta}{2} |11\rangle_L - \sin \frac{\theta}{2} e^{i\phi} |a_4\rangle$. The only nonzero element of $U(4)$ -valued connection is $A_{33} = -\sin^2 \frac{\theta}{2} \dot{\phi}$. When the dark states evolve adiabatically along a cyclic closed path, the logical basis $|11\rangle_L$ will acquire a Berry's phase β_1 , while the other computational

components $|00\rangle_L$, $|01\rangle_L$, and $|10\rangle_L$ are decoupled. The associated two-qubit CP gate is given by $U_{cz} = e^{i\beta_1 |11\rangle_L\langle 11|}$ in DFS. In our implementation, there is no need to apply four-body interactions, just two-body ones. One can see that the adiabatic two-qubit holonomy can be accelerated effectively, as illustrated in the implementation for speeding up single-logical-qubit adiabatic phase gate in DFS. Actually, this is the main advantage of our work, different from previous works. The combination of this accelerated two-qubit holonomic CP gate and the two noncommuting accelerated single-qubit holonomic gates in DFS described earlier suggests that the complete set of shortcuts to adiabatic holonomic quantum gates in DFS are effectively built along with a realisable implementation based on four-NV-center systems.

Intuitively, the present scheme can be scaled up the encoded logical qubits easily as it requires only two-body interactions. For example, if we want to design the two-logic-qubit holonomic CP gate between the m -th and n -th logical qubits, the target Hamiltonian has the same form as Eq. (11) but with the exchanging $\lambda'_{1,2} \rightarrow \lambda'_{4m-3,4m-2}$ and $\lambda'_{1,3} \rightarrow \lambda'_{4m-3,4m-1}$. Also, we can realize the shortcuts for this scalable CP gate by using the approach discussed above.

Generally, speeding up holonomic quantum gates inevitably leads to at least an extra transition or detunings because of the existence of the additional Hamiltonian. By taking the choice of the special path along the geodesic curve, the controlled complexity can be greatly reduced and the operation procedures can also be largely simplified. For example, in the Bloch space, choosing the evolution trajectories of the shortcuts to two noncommuting adiabatic holonomic single-qubit gates and a two-qubit CP gate on DFS are connected geodesic curves, one can obtain that the dynamical phases of evolution path are vanishing, thus the set of the accelerated adiabatic holonomic quantum gates are pure geometric. Meanwhile, in the whole steps, a feasible route is exploited to make sure that all of the elements of matrix-valued connection A are vanishing, i.e., $A_{kl}^n = 0$.

VI. DISCUSSION AND SUMMARY

For N identical NV centers placed near the microsphere cavity surface, the coupling strength between them can be expressed in terms of the NV and cavity parameters as $G = \Gamma_0 |\vec{E}(r)/\vec{E}_{max}| \sqrt{V_a/V_m}$ [61], in which Γ_0 donates the spontaneous decay rate of the excited state $|e\rangle$ for the NV center, $|\vec{E}(r)/\vec{E}_{max}|$ is the normalized electric field strength at the location r , $V_a = 3c^3/4\pi\nu^2\Gamma_0$ serves as a characteristic interaction volume with c being the speed of light and ν being the transition frequency between the excited state $|e\rangle$ and the ground state $|0\rangle$, and V_m is the cavity mode volume. The spontaneous decay rate Γ_0 of the excited state reported in experiment is $2\pi \times 83$ MHz [62, 63]. Considering $|\vec{E}(r)/\vec{E}_{max}| = 1/6$, $\nu = 471$ THz (the transition wavelength between states $|e\rangle$ and $|0\rangle$ is 637 nm), and $V_m = 100 \mu\text{m}^3$, we obtain $G \approx 2\pi \times 1$ GHz [54]. The dephasing time of up to 0.65 ms for pure NV centers has been experimentally observed [64]. When dynamical decoupling pulse sequences are employed to suppress nitrogen-

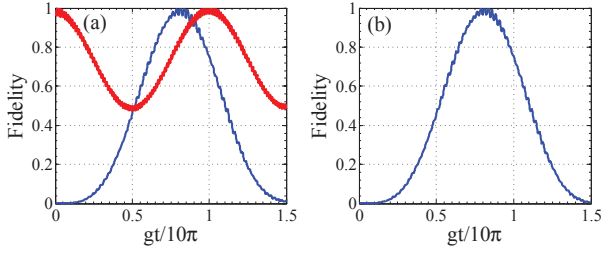


FIG. 2: (a) The fidelities of shortcuts to single-qubit holonomic phase (blue line) and bit-phase (red line) gates with the initial state $\frac{1}{\sqrt{2}}(|0\rangle_L + |1\rangle_L)$, and $|0\rangle_L$, respectively. (b) The fidelity of shortcuts to two-qubit holonomic CP gate with the initial state $\frac{1}{\sqrt{2}}(|00\rangle_L + |11\rangle_L)$. Here, $g = 2\pi \times 50$ MHz, the decay rate of microsphere cavity is $\kappa = 2\pi \times 0.0748$ MHz [51], and the relaxation and dephasing rates of NV centers are $\gamma = \gamma_\varphi = 2\pi \times 4$ KHz [64].

vacancy spin decoherence, the dephasing time of NV centres can reach 0.6 s at 77 K [65]. On the other hand, the cavity frequency is $\omega_c = 2\pi \times 74.8$ THz with the decay rate $\kappa = 2\pi \times 0.0748$ MHz and the quality factor $Q = 10^9$ [51]. The transition frequencies of NV centers are $\omega_{10} = 2.87$ GHz (zero field splitting) and $\omega_{e0} = 471$ THz with a zero-phonon line at 1.945 eV [66]. Here, we have $\omega_{10} \ll \omega_c$, and the detuning δ_j is dependent on the difference between the cavity frequency ω_c and the external laser field frequency $\omega_{L,j}$. Choosing different frequency of classical laser field, we can obtain the required different detuning δ_j when the cavity frequency is fixed. In our implementation, the coupling strength between the NV center and the laser field could be $\Omega_L = 2\pi \times 500$ MHz, and the detuning is $\Delta = 2\pi \times 20$ GHz which satisfies the conditions $\Delta \gg G$ and $\Delta \gg \Omega_L$ to ensure that the excited state $|e\rangle$ can be eliminated adiabatically. On the other hand, assuming $\Delta \gg \delta$, e.g., $\delta = 2\pi \times 2$ GHz, we have $g \approx 2G\Omega_L/\Delta = 2\pi \times 50$ MHz that fulfills the large detuning condition $\delta \gg g$. This guarantees there is no energy exchange between the NV systems and the microcavity. Indeed, it is not necessary to apply the condition $\Delta \gg \delta$, and we can also reach the condition of $\delta \gg g$ provided the order of magnitude of Δ or δ is not less than GHz, irrespective of the relation between them. Consequently, we can gain the different effective Rabi frequencies $\lambda'_{j,k}$ by tuning the detuning between the cavity frequency and the external laser field frequency. Once the cavity frequency and the initial phase of the external laser field are determined, it is easy to realize the entire physical procedures required in the shortcuts to adiabatic HQC in DFS by changing the external laser field frequency $\omega_{L,j}$.

Assuming all the qubits are in the collective dephasing environment, we use the Lindblad master equation to simulate the performance of the quantum gates under the influence of dissipation [67]:

$$\frac{d\rho}{dt} = -i[H_{int}, \rho] + \kappa D[a]\rho + \gamma D[S^-]\rho + \gamma_\varphi D[S^z]\rho, \quad (12)$$

where H_{int} donates the Hamiltonian in the form of Eq. (4), ρ is the density matrix operator, $D[L]\rho = (2L\rho L^\dagger - L^\dagger L\rho -$

$\rho L^\dagger L)/2$. $S^- = \sum_{i=1} \sigma_i^-$ and $S^z = \sum_{i=1} \sigma_i^z$. γ and γ_φ are the collective relaxation rate and dephasing rate of NV centers, respectively. κ is the decay rate of the cavity. Here, we define the fidelity of the gate by $F = \langle \psi_{ideal} | \rho | \psi_{ideal} \rangle$ with $|\psi_{ideal}\rangle$ being the corresponding ideally final state under an ideal gate operation on its initial state $|\psi_{in}\rangle$. Numerical simulation of the fidelities for shortcuts to single-qubit holonomic phase, bit-phase and two-qubit CP gates are shown in Fig. 2(a) and Fig. 2(b) with initial states $\frac{1}{\sqrt{2}}(|0\rangle_L + |1\rangle_L)$, $|0\rangle_L$ and $\frac{1}{\sqrt{2}}(|00\rangle_L + |11\rangle_L)$, respectively. By taking the feasible experimental parameters as $\delta_1 = 2\pi \times 4$ GHz, $\delta_2 = 2\pi \times 0.4$ GHz, and $\delta_3 = 2\pi \times 0.4$ GHz, the fidelities of single-qubit holonomic phase and two-qubit CP gates can reach about 99.52% and 99.76%, respectively. Moreover, we numerically get a high fidelity of 99.91% for single-qubit holonomic bit-phase gate with the detunings between the frequencies of microsphere cavity and NV centers being $\delta_1 = 2\pi \times 7$ GHz, $\delta_2 = 2\pi \times 0.7$ GHz, $\delta_3 = 2\pi \times 0.7$ GHz, and $\delta_4 = 2\pi \times 0.7$ GHz. That is, our robust protocol has a feasible physical implementation with the current experimental techniques.

In summary, we have proposed an efficient scheme for the shortcuts to HQC in DFS by employing TQDA. Combining the features of HQC and DFS, the present protocol is robust against the local fluctuations and collective noises. The optimized Hamiltonian of TQDA can greatly shorten the time required in the adiabatic HQC to avoid the errors due to the long runtime of quantum information processing. Moreover, we give a feasible physical implementation of this scheme on diamond NV centers large-detuned interacting with a quantized WGM of a microsphere cavity. Our scheme can also be extended to multi-logic-qubit HQC in DFS efficiently. Compared with previous works, our scheme has the following advantages: First, the TQDA is newly applied to implement universal HQC in DFS, and we realize shortcuts to both two noncommuting single-qubit holonomic gates and a two-qubit holonomic CP gate in DFS. This provides the necessary shortcuts for the universal HQC in DFS. Second, this protocol does not require four-body interactions and the entire quantum operation procedures for realizing the shortcuts to universal adiabatic holonomic quantum gates in DFS are performed by a virtual photon process, thus the experimental challenge is much reduced. Third, our calculation indicates that our physical implementation proposal can be efficiently realized by appropriately applying the external laser pulses as long as the initial conditions are determined, which greatly simplifies the experimental complexity. Numerical calculations reveal that the present scheme can reach a high fidelity with current technology, which may offer a feasible route towards robust HQC.

ACKNOWLEDGES

The author Xue-Ke Song would like to thank Dr. J. Zhou for helpful discussion. Fu-Guo Deng was supported by the National Natural Science Foundation of China under Grant No. 11474026 and the Fundamental Research Funds for the Central Universities under Grant No. 2015KJJC01.

Qing Ai was supported by National Natural Science Foundation of China under Grant No. 11505007, the Youth Scholars Program of Beijing Normal University under Grant No.

2014NT28, and the Open Research Fund Program of the State Key Laboratory of Low-Dimensional Quantum Physics, Tsinghua University under Grant No. KF201502.

-
- [1] Nielsen M A and Chuang I L 2000 *Quantum Computation and Quantum Information*, Cambridge University Press, Cambridge, UK
- [2] Cirac J I and Zoller P 1995 *Phys. Rev. Lett.* **74** 4091
- [3] Saffman M, Walker T G, and Mølmer K 2010 *Rev. Mod. Phys.* **82** 2313
- [4] Knill E, Laflamme R, and Milburn G J 2001 *Nature (London)* **409** 46
- [5] Ren B C and Deng F G 2014 *Sci. Rep.* **4** 4623
- [6] Li X Q, Wu Y W, Steel D, Gammon D, Stievater T H, Katzer D S, Park D, Piermarocchi C, and Sham L J 2003 *Science* **301** 809
- [7] Blais A, Huang R S, Wallraff A, Girvin S M, and Schoelkopf R J 2004 *Phys. Rev. A* **69** 062320
- [8] Zanardi P and Rasetti M 1999 *Phys. Lett. A* **264** 94
- [9] Pachos J, Zanardi P, and Rasetti M 2000 *Phys. Rev. A* **61** 010305(R)
- [10] Duan L M, Cirac J I, and Zoller P 2001 *Science* **292** 1695
- [11] Zhu S L and Wang Z D 2002 *Phys. Rev. Lett.* **89** 097902
- [12] Xu G F, Zhang J, Tong D M, Sjöqvist E, and Kwek L C 2012 *Phys. Rev. Lett.* **109** 170501
- [13] Sjöqvist E, Tong D M, Andersson L M, Hessmo B, Johansson M, and Singh K 2012 *New J. Phys.* **14** 103035
- [14] Spiegelberg J and Sjöqvist E 2013 *Phys. Rev. A* **88** 054301
- [15] Mousolou V A, Canali C M, and Sjöqvist E 2014 *New J. Phys.* **16** 013029
- [16] Zhang J, Kwek L C, Sjöqvist E, Tong D M, and Zanardi P 2014 *Phys. Rev. A* **89** 042302
- [17] Liang Z T, Du Y X, Huang W, Xue Z Y, and Yan H 2014 *Phys. Rev. A* **89** 062312
- [18] Xu G F and Long G L 2014 *Phys. Rev. A* **90** 022323
- [19] Xu G F and Long G L 2014 *Sci. Rep.* **4** 6814
- [20] Zhou J, Yu W C, Gao Y M, and Xue Z Y 2015 *Opt. Express* **23** 014027
- [21] Xue Z Y, Zhou J, and Wang Z D 2015 *Phys. Rev. A* **92** 022320
- [22] Zhu S L and Wang Z D 2003 *Phys. Rev. Lett.* **91** 187902
- [23] Zheng S B 2004 *Phys. Rev. A* **70** 052320
- [24] Feng X L, Wu C F, Sun H, and Oh C H 2009 *Phys. Rev. Lett.* **103** 200501
- [25] Feng G R, Xu G F, and Long G L 2013 *Phys. Rev. Lett.* **110** 190501
- [26] Abdumalikov Jr A A, Fink J M, Juliusson K, Pechal M, Berger S, Wallraff A, and Filipp S 2013 *Nature (London)* **496** 482
- [27] Arroyo-Camejo S, Lazariev A, Hell S W, and Balasubramanian G 2014 *Nat. Commun.* **5** 4870
- [28] Zu C, Wang W B, He L, Zhang W G, Dai C Y, Wang F, and Duan L M 2014 *Nature (London)* **514** 72
- [29] Zanardi P and Rasetti M 1997 *Phys. Rev. Lett.* **79** 3306
- [30] Duan L M and Guo G C 1998 *Phys. Rev. A* **57** 737
- [31] Lidar D A, Chuang I L, and Whaley K B 1998 *Phys. Rev. Lett.* **81** 2594
- [32] Kwiat P G, Berglund A J, Altepeter J B, and White A G 2000 *Science* **290** 498
- [33] Mohseni M, Lundeen J S, Resch K J, and Steinberg A M 2003 *Phys. Rev. Lett.* **91** 187903
- [34] Ollerenshaw J E, Lidar D A, and Kay L E 2003 *Phys. Rev. Lett.* **91** 217904
- [35] Wu L A, Zanardi P, and Lidar D A 2005 *Phys. Rev. Lett.* **95** 130501
- [36] Zhang X D, Zhang Q H, and Wang Z D 2006 *Phys. Rev. A* **74** 034302
- [37] Cen L X, Wang Z D, and Wang S J 2006 *Phys. Rev. A* **74** 032321
- [38] Oreshkov O, Brun T A, and Lidar D A 2009 *Phys. Rev. Lett.* **102** 070502
- [39] Berry M V 2009 *J. Phys. A: Math. Theor.* **42** 365303
- [40] Demirplak M, and Rice S A 2003 *J. Phys. Chem. A* **107** 9937
- [41] Demirplak M, and Rice S A 2005 *J. Phys. Chem. B* **109** 6838
- [42] Chen X, Lizuain I, Ruschhaupt A, Guéry-Odelin D, and Muga J G 2010 *Phys. Rev. Lett.* **105** 123003
- [43] del Campo A 2013 *Phys. Rev. Lett.* **111** 100502
- [44] Moliner M, and Schmitteckert P 2013 *Phys. Rev. Lett.* **111** 120602
- [45] Giannelli L, and Arimondo E 2014 *Phys. Rev. A* **89** 033419
- [46] Bason M G, Viteau M, Malossi N, Huillery P, Arimondo E, Ciampini D, Fazio R, Giovannetti V, Mannella R, and Morsch O 2012 *Nat. Phys.* **8** 147
- [47] Zhang J, Shim J H, Niemeyer I, Taniguchi T, Teraji T, Abe H, Onoda S, Yamamoto T, Ohshima T, Isoya J, and Suter D 2013 *Phys. Rev. Lett.* **110** 240501
- [48] Zhang J, Kyaw T H, Tong D M, Sjöqvist E, and Kwek L C 2015 *Sci. Rep.* **5** 18414
- [49] Pyshkin P V, Luo D W, Jing J, You J Q, and Wu L A 2015 arXiv:1507.00815
- [50] Hanson R, Gywat O, and Awschalom D D 2006 *Phys. Rev. B* **74** 161203(R)
- [51] Vernooij D M, Ilchenko V S, Mabuchi H, Streed E W, and Kimble H J 1998 *Opt. Lett.* **23** 247
- [52] Armani D K, Kippenberg T J, Spillane S M, and Vahala K J 2003 *Nature (London)* **421** 925
- [53] Park Y S, Cook A K, and Wang H L 2006 *Nano. Lett.* **6** 2075
- [54] Yang W L, Xu Z Y, Feng M, and Du J F 2010 *New J. Phys.* **12** 113039
- [55] Wei H R and Deng F G 2013 *Phys. Rev. A* **88** 042323
- [56] Ren B C, Wang G Y, and Deng F G 2015 *Phys. Rev. A* **91** 032328
- [57] Liu Q and Zhang M 2015 *Phys. Rev. A* **91** 062321
- [58] Santori C, Tamarat P, Neumann P, Wrachtrup J, Fattal D, Beausoleil R G, Rabeau J, Olivero P, Greentree A, Prawer S, Jelezko F, and Hemmer P 2006 *Phys. Rev. Lett.* **97** 247401
- [59] Tamarat P, Gaebel T, Rabeau J R, Greentree A D, Wilson H, Hollenberg L C L, and Prawer S 2006 *Phys. Rev. Lett.* **97** 083002
- [60] Acosta V M, Santori C, Faraon A, Huang Z, Fu K M C, Stacey A, Simpson D A, Ganesan K, Tomljenovic-Hanic S, Greentree A D, Prawer S, and Beausoleil R G 2012 *Phys. Rev. Lett.* **108** 206401
- [61] Spillane S M, Kippenberg T J, Vahala K J, Goh K W, Wilcut E, and Kimble H J 2005 *Phys. Rev. A* **71** 013817
- [62] Batalov A, Zierl C, Gaebel T, Neumann P, Chan I Y, Balasubramanian G, Hemmer P R, Jelezko F, and Wrachtrup J 2008 *Phys. Rev. Lett.* **100** 077401
- [63] Neumann P, Kolesov R, Jacques V, Beck J, Tisler J, Batalov

- A, Rogers L, Manson N B, Balasubramanian G, Jelezko F, and Wrachtrup J 2009 *New J. Phys.* **11** 013017
- [64] Mizuochi N, Neumann P, Rempp F, Beck J, Jacques V, Siyushev P, Nakamura K, Twitchen D J, Watanabe H, Yamasaki S, Jelezko F, Wrachtrup J 2009 *Phys. Rev. B* **80** 041201(R)
- [65] Bar-Gill N, Pham L M, Jarmola A, Budker D, and Walsworth R L 2013 *Nat. Commun.* **4** 1743
- [66] Childress L, Gurudev Dutt M V, Taylor J M, Zibrov A S, Jelezko F, Wrachtrup J, Hemmer P R, and Lukin M D 2006 *Science* **314** 281
- [67] Lindblad G, 1976 *Commun. Math. Phys.* **48** 119